The Long Acidic Tail of High Mobility Group Box 1 (HMGB1) Protein Forms an Extended and Flexible Structure That Interacts with Specific Residues within and between the HMG Boxes†

Stefan Knapp,‡ Susanne Müller,§ Giuseppe Digilio,|| Tiziana Bonaldi,§ Marco E. Bianchi,⊥ and Giovanna Musco*,#

Discovery Research Oncology, Department of Chemistry, Pharmacia Corporation, Viale Pasteur 10, 20014 Nerviano, Italy, San Raffaele Scientific Institute, via Olgettina 58, 20132 Milano, Italy, Bioindustry Park del Canavese Spa, Via Ribes 5, 10010 Colleretto Giacosa, Italy, San Raffaele University, via Olgettina 58, 20132 Milano, Italy, and Dulbecco Telethon Institute, c/o San Raffaele Scientific Institute, Via Olgettina 58, 20132 Milano, Italy

Received April 1, 2004; Revised Manuscript Received July 5, 2004

ABSTRACT: HMGB1 (high mobility group B1) is a conserved chromosomal protein composed of two similar DNA binding domains (HMG box A and box B) linked by a short basic stretch to an acidic C-terminal tail of 30 residues. The acidic tail modulates the DNA binding properties of HMGB1, and its length differentiates the various HMGB family members. We synthesized a peptide that corresponds to the acidic tail in HMGB1 (T-peptide) and studied its binding to the single boxes and to the fragment corresponding to tailless HMGB1 (designated as AB_{bt} fragment). CD spectroscopy showed that T-peptide stabilizes significantly the AB_{bt} fragment and that the complex has an identical thermal stability as full-length HMGB1. Calorimetric and NMR data showed that T-peptide binds with a dissociation constant of 9 μM to box A and much more weakly to box B. $^{1}H-^{15}N$ HSQC spectra of full-length HMGB1 and of the AB_{bt} fragment are very similar; the small chemical shift differences that exist correspond to those residues of the AB_{bt} fragment that were affected by the addition of the T-peptide. We conclude that the T-peptide mimics closely the acidic tail and that the basic stretch and the acidic tail form an extended and flexible segment. The tail interacts with specific residues in the boxes and shields them from other interactions.

HMGB1[1] is an abundant and highly conserved non-histone chromosomal protein, which binds without sequence specificity to the minor groove of DNA, causing local distortions in the DNA structure (*1*). In addition, HMGB1 associates with high affinity to DNA with highly bent structures, such as four-way junctions and cisplatin-modified DNA (*1*). HMGB1 plays a crucial role in the regulation of transcription either by remodeling chromatin and nucleosome structure or through direct interaction with transcription factors such as Hox, steroid hormone receptors, p53, NF-κB, and TBP (*2*). The functional importance of HMGB1 as a regulator of transcription in vivo has been confirmed by the phenotype of the HMGB1 knockout mouse, which dies shortly after birth due to hypoglycemia and shows a defect in the transcriptional function of the glucocorticoid receptor (*3*). Recent studies have revealed that HMGB1 has also important functions outside the cell, where it acts as a cytokine (*4*, *5*) and is a ligand for a membrane receptor, RAGE (*6*, *7*).

HMGB1 has a tripartite domain organization: it contains two similar DNA binding domains, the HMG boxes A and B, each around 75 amino acids in length, connected by a short linker region and followed by a short basic linker and an acidic tail formed by 30 consecutive glutamate and aspartate residues. The structure of the single boxes of HMGB1 has been characterized in detail (*8*−*11*); their global fold, despite the low sequence identity (29%), is rather conserved and is composed of three α-helices (I−III) arranged in an L-like shape and stabilized by two hydrophobic cores. However, despite their similarity, several important structural and functional differences between the two HMG boxes have been observed. Box A differs significantly from box B in the relative orientations of helices I and II and in the trajectory of the helix I−II loop. Furthermore, the two boxes have distinct electrostatic surface potentials in their DNA binding regions, which might account for differences observed in interaction with DNA, such as the degree of bending introduced upon binding to DNA and the affinity for four-way junctions.

† S.M. is a recipient of the EMBO Restart Fellowship. The Italian Ministry of Education, University and Research funded M.E.B. (COFIN 2001) and G.M. (FIRB Grant RBAU01L9J9). G.M. also received funding from Telethon.

* Author for correspondence. Tel: +39-0226434824. Fax: +39-0226434153. E-mail: musco.giovanna@hsr.it.

‡ Pharmacia Corp.

§ San Raffaele Scientific Institute.

|| Bioindustry Park del Canavese Spa.

⊥ San Raffaele University.

Dulbecco Telethon Institute.

[1] Abbreviations: ΔCS, composite chemical shift displacement vector; AB_{bt}, tailless HMGB1, including box A, box B, and the basic linker region (residues 1−187); box A, domain A of HMGB1 (residues 1−89); box B, domain B of HMGB1 (residues 90−175); CD, circular dichroism; ITC, isothermal titration calorimetry; HMGB1, high mobility group protein B1; HSQC, heteronuclear single-quantum coherence; NMR, nuclear magnetic resonance; NOESY, nuclear Overhauser effect spectroscopy; T-peptide, synthetic peptide corresponding to residues 185−214 of HMGB1.

10.1021/bi049364k CCC: $27.50 © 2004 American Chemical Society
Published on Web 09/02/2004

NMR (*12*) and calorimetric studies (*13*) have shown that the two boxes A and B behave as rigid structures that do not interact when connected by the linker region. However, thermodynamic studies showed that in the full-length protein stabilizing interactions occur between the acidic tail and at least one of the boxes (*13*).

In full-length HMGB1, the acidic tail has important functional roles. It modulates the interaction with DNA and its helix-distorting ability (*14*−*16*), is required for preferential binding to DNA minicircles relative to linear DNA (*17*), and modulates the interaction with nucleosomes and chromatin remodeling machines (*18*, *19*). Finally, the tail modulates the acetylation of HMGB1 by histone acetyltransferases (*20*); in turn, HMGB1 acetylation is essential for its secretion by activated myeloid cells (*21*).

Recently, cross-linking experiments have shown that the acidic tail interacts with the boxes, in particular with box B(*22*). At present there is no structural information available on how the acidic tail interacts with the two boxes. In this study we used a free 30-residue peptide (T-peptide, residues 185−214 of HMGB1) as a model of the acidic tail. Binding of the T-peptide to tailless HMGB1 was characterized using titration calorimetry (ITC) as well as CD spectroscopy, and interacting residues were identified by two-dimensional heteronuclear NMR spectroscopy. Our study reveals that the T-peptide mimics very well the interaction pattern of the acidic tail in the context of full-length HMGB1. This interaction is very dynamic, but the acidic tail will be in close proximity to the boxes most of the time, shielding them from other interactions. Furthermore, our studies reveal that all residues outside the two HMG boxes (including the ones that interact with RAGE) are unstructured and flexible.

EXPERIMENTAL PROCEDURES

Cloning, Expression, and Purification of Proteins. Uniformly ^{15}N-labeled and ^{15}N,^{13}C-labeled proteins were prepared by growing the *Escherichia coli* strain BL21(DE3) overexpressing the HMGB1 constructs in minimal medium containing $^{15}NH_4Cl$, with or without [^{13}C]glucose. The recombinant proteins were purified as described (*16*). The constructs used were box A (residues 1−89), box B (residues 90−175), fragment AB_{bt} (residues 1−187), and full-length HMGB1. T-peptide was synthesized by solid-phase synthesis and subsequently purified by reverse-phase HPLC. The purity and molecular weight of T-peptide were verified using electrospray mass spectrometry.

CD Spectroscopy. CD spectra were recorded using an AVIV 252 CD spectrophotometer and software provided by the manufacturer. Cuvettes with a 0.1 cm path length were used. Each spectrum was averaged using four accumulations collected in 1 nm intervals with an averaging time of 10 s. Temperature melting curves were recorded at 222 nm in kinetic mode using a temperature ramp of 1 °C/min. The protein concentration was 2 μM.

NMR Spectroscopy. NMR spectra were acquired at 293 K on a Bruker Avance 600 NMR spectrometer equipped with inverse triple-resonance probes and pulsed-field gradients. Spectra were processed with NMRpipe (*23*) and analyzed using XEASY (*24*). The ^{1}H, ^{13}C, ^{15}N assignment of the backbone resonances of the different HMGB1 fragments was obtained from constant time HNCA (*25*) and HNCACB (*26*) with water-flip-back modifications (*27*) and CBCA(CO)NH (*28*) with WATERGATE (*29*), using uniformly ^{15}N,^{13}C-labeled samples.

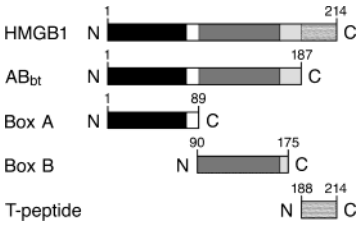

FIGURE 1: Schematic representation of the proteins used in this study. Numbers indicate the first and last amino acid residue. HMG box A comprises approximately aa 4−80 (black), HMG box B aa 90−165 (dark gray), and the acidic tail aa 185−214 (gray). The linker between box A and box B is in white, and the basic stretch between box B and the tail is in light gray.

For the titration of the different HMGB1 fragments with T-peptide, typical protein concentrations were 0.3 mM in 10 mM phosphate buffer (pH 5), 150 mM NaCl, and 10 mM DTT. To minimize dilution and NMR signal loss, titrations were carried out by adding small quantities of a concentrated (10 mM) T-peptide stock to the NMR samples. For each titration point a two-dimensional water-flip-back ^{15}N-edited HSQC spectrum was recorded at 293 K. The ^{15}N-edited HSQC data were recorded as 512 (100) complex points, with 55 ms (60 ms) acquisition times, apodized by 60 shifted squared (sine) window functions, and zero filled to 1024 (512) points for ^{1}H (^{15}N), respectively. Assignments of the corresponding amide groups in the complex AB_{bt}−T-peptide were made by following individual cross-peaks through a titration series.

For each residue the composite chemical shift displacement vector ΔCS was calculated as $[\Delta\delta^2HN + \Delta\delta^2N/25]^{1/2}$.

Figure 6 was generated using ICM (*30*). The model of boxes A and B (PDB entries 1aab and 1hme) connected by their linker has been built and minimized with the BIOPOLYMER and DISCOVER_3 modules of INSIGHTII (Accelrys, San Diego).

Isothermal Titration Calorimetry. Calorimetric measurements were carried out using a VP-ITC titration calorimeter from MicroCal Inc. Samples were extensively dialyzed against 50 mM sodium phosphate, pH 7.5, 150 mM NaCl, and 1 mM DTT. All solutions were carefully degassed before the titrations using equipment provided with the calorimeter. Each titration experiment consisted of a first (5 μL) injection of T-peptide (400 μM) followed by 10 μL injections into a solution of HMGB1 fragments (25 μM). Heats of dilution were measured in blank titrations by injecting T-peptide into the buffer and were subtracted from the binding heats. Data were analyzed using a single binding site model implemented in the Origin software package provided with the instrument.

RESULTS

The Acidic Tail Stabilizes the HMG Boxes both When It Is Connected to Them and When It Is Disconnected. The polypeptides used in this study are shown in Figure 1 and were purified as described in Experimental Procedures. In particular, AB_{bt} represents HMGB1 minus the acidic tail. To understand the mechanism of the interaction of the acidic tail within HMGB1, we chemically synthesized a peptide

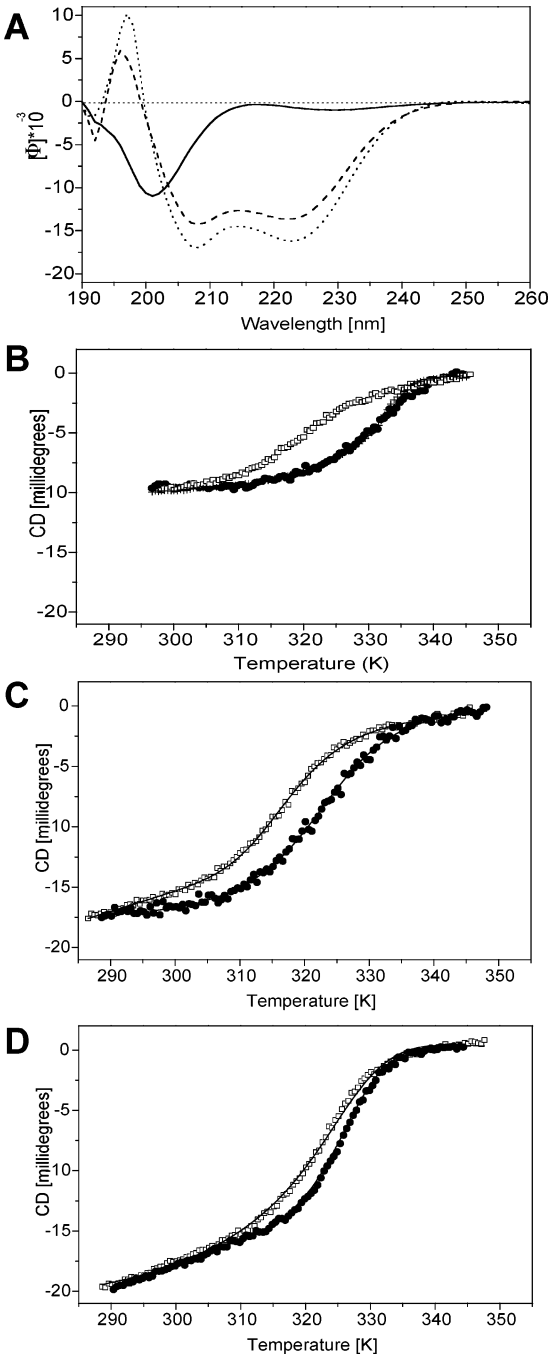

FIGURE 2: CD spectroscopy. (A) CD spectra of HMGB1 (dotted line), AB_{bt} (dashed line), and T-peptide (solid line). (B) Melting curves of AB_{bt} (open squares), of AB_{bt} plus T-peptide in a 1:2 molar ratio (crosses), and of full-length HMGB1 (filled dots). The data were recorded at 222 nm. Refolding of AB_{bt} in the presence and absence of T-peptide was partially reversible under these conditions (20 mM sodium phosphate, pH 7.4, 30 mM NaCl). The melting curve of full-length HMGB1 superimposes completely with the curve of the AB_{bt}−T-peptide complex, indicating that the stabilizing effect of the T-peptide on AB_{bt} is similar to that of the acidic tail in the full-length protein. (C) Melting curve of box A (open squares) and box A plus T-peptide in a 1:2 molar ratio (filled dots). (D) Melting curve of box B (open squares) and box B plus T-peptide in a 1:2 molar ratio (filled dots).

(T-peptide) that corresponds to the 30 amino acid long acidic tail of HMGB1 (residues 185−214).

The secondary structures of the T-peptide, the AB_{bt} fragment, and full-length HMGB1 were probed using circular dichroism (CD) spectroscopy (Figure 2A). As expected, the

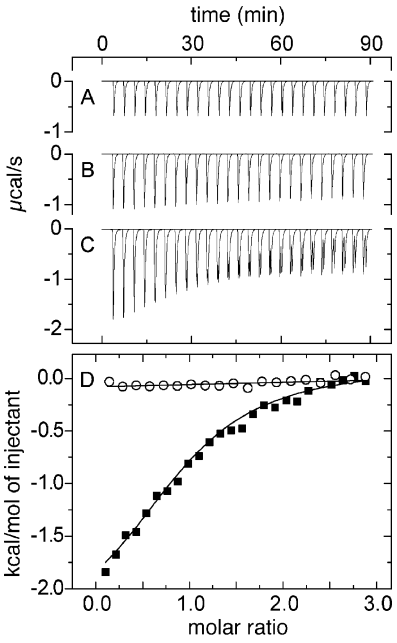

FIGURE 3: Binding of the T-peptide to HMG boxes A and B measured by ITC. The top panel shows the raw heat data obtained over a series of injections of T-peptide into buffer (trace A), box B (trace B), and box A (trace C). Titrations were performed in PBS at 20 °C. The lower panel shows the binding isotherms; solid squares refer to box A (line represents the nonlinear least squares best fit). For box B (open circles), a line has been drawn only to guide the eye. Binding parameters determined for box A were $K_A = (1.15 \pm 0.14) \times 10^5\ M^{-1}$, $\Delta H_{obs} = -2.6 \pm 0.15$ kcal/mol, $T\Delta S_{obs} = 4.2$ kcal/mol, and stoichiometry $n = 0.95$.

spectra indicated that T-peptide is a random coil whereas both AB_{bt} and HMGB1 are predominantly α-helical.

We then used ellipticity at 222 nm (a measure of α-helical structure) to probe the thermal stability of AB_{bt} and HMGB1 (Figure 2B). The denaturation of HMGB1, and of the AB_{bt} fragment in both the presence and absence of the T-peptide, is partially reversible and does not allow the precise calculation of thermodynamic stability data. Fragment AB_{bt} has a melting temperature of 322 K (49 °C), and the addition of T-peptide increases it by 12 K. Full-length HMGB1 has a melting temperature of 334 K (61 °C), identical to that of the complex between AB_{bt} and T-peptide. This indicates that the complex between the T-peptide and AB_{bt} mimics very closely the thermostability of full-length HMGB1.

Similar thermostability studies were performed on single boxes, with and without T-peptide (Figure 2C,D). The melting temperature of box A is shifted by 7 K (from 315 to 322 K), whereas that of box B is shifted only by 2.5 K (from 325 to 327 K). Thus, the T-peptide stabilizes both individual boxes, with a larger effect on box A.

The T-Peptide Binds to Box A. The association constant determined by isothermal titration calorimetry (ITC) of T-peptide with box A was $(1.1 \pm 0.14) \times 10^5\ M^{-1}$ ($K_D = 9\ \mu M$) (Figure 3, trace C). The ITC tracings are typical for a weak interaction. The stoichiometry is close to 1:1. The interaction at 293 K is favorable both enthalpically ($\Delta H_{obs} = -2.6 \pm 0.15$ kcal/mol) and entropically ($T\Delta S_{obs} = 4.2$ kcal/mol). The negative binding enthalpy suggests the existence of favorable polar interactions. Sedimentation equilibrium experiments confirmed that the complex between box A and the T-peptide has a mass of16 ± 2 kDa,

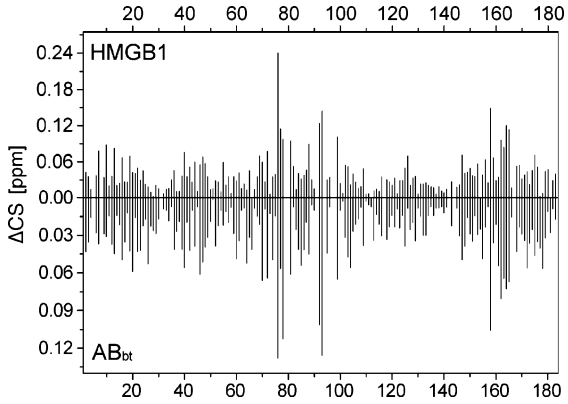

FIGURE 4: Chemical shift differences. Histograms showing the value of the chemical shift displacement vector ΔCS between HMGB full length and AB_{bt} (HMGB1) and between AB_{bt} and AB_{bt}−T-peptide (1:4) (AB_{bt}). Numbers on the *x*-axis indicate the residue in the HMGB1 sequence. Note that the two panels are arranged symmetrically about the *y*-axis.

compatible with the formation of a strong 1:1 complex (data not shown).

No binding of the T-peptide to box B was detected by ITC (Figure 3, traces B and D), suggesting that the interaction is too weak to be detected using calorimetric methods.

Mapping of the Box Residues Interacting with the T-Peptide. To identify the box residues involved in the interaction with the T-peptide, we used chemical shift perturbation methods.

The $^1H-^{15}N$ HSQC spectrum of the AB_{bt} fragment is essentially the sum of the HSQC spectra of the two independent HMG box domains (data not shown). This confirms that the two boxes, when linked in the entire HMGB1 protein, maintain their fold and behave as structurally independent domains, as already shown (*12*). The secondary structure of the amino acids belonging to the basic region downstream of box B was assessed using Cα secondary chemical shifts and ^{15}N NOESY-HSQC experiment. Both methods indicate that this amino acid stretch is unstructured: ΔCα chemical shifts are negative and the NOEs typical of α-helices and *β*-sheets are absent (data not shown).

T-peptide was then titrated into the solution of ^{15}N-labeled AB_{bt} fragment, and chemical shift differences (ΔCS) were monitored by recording a series of $^1H-^{15}N$ HSQC spectra. Chemical shift differences were small, suggesting that the conformational changes of the AB_{bt} fragment upon binding of the T-peptide are small. This facilitated residue assignment in the complex. Most chemical shift changes were a continuous and monotonic function of the amount of added T-peptide (up to a 1:4 protein:peptide ratio), indicative of a fast-exchange regime on the NMR time scale. However, at substoichiometric ratios we observed line broadenings for the peaks corresponding to T76, I78, and I158, indicative of an intermediate exchange regime. The residues showing the largest ΔCS are T76 and I78 in box A and N92, A93, I158, and R162 in box B, as shown in the lower part of Figure 4. Several nearby residues (Y70, R72, and K81 in box A and A163, K164, and G165 in box B) are also affected to a lower extent.

T-peptide was similarly titrated into solutions of ^{15}N-labeled box A and box B. The residues showing significant chemical shift changes were again T76 and I78 in box A and N92, A93, I158, and R162 in box B (data not shown). When mapped on the structures of boxes A and B (*9*, *11*), these residues cluster to the C-terminus of box A and to the N- and C-termini of box B. Interestingly, despite the large number of positively charged residues on helix III of both boxes, only the chemical shift of R72 is affected in a minor way by the presence of the acidic tail, suggesting that the interactions between both boxes and the T-peptide are not simply a result of a nonspecific electrostatic attraction.

The interaction of the T-peptide with box A reaches saturation at a stoichiometry of 3:1 (T-peptide:box A), whereas the interaction with box B does not reach saturation up to a 5-fold excess of T-peptide (data not shown). This result is in agreement with the ITC and thermostability data indicating that the interaction of the T-peptide with box B is much weaker than with box A.

The Acidic Tail Interacts with the HMG Boxes in the Full-Length HMGB1 Protein. We next recorded the $^1H-^{15}N$ HSQC spectrum of full-length HMGB1 (Figure 5A). This is very similar to that of the AB_{bt} fragment, indicating that the global conformation is maintained. The residues in the acidic tail have typical random coil frequencies, with sharp and intense peaks. Individual tail residues could not be assigned: the corresponding peaks are fewer than expected because of spectral overlap and exchange with the solvent.

Despite the high similarity between the spectra of full-length HMGB1 and of AB_{bt}, chemical shift differences were observed for residues T76, I78, N92, A93, I158, and R162 (Figure 4). Remarkably, these are the backbone NH frequencies which are most affected upon addition of the T-peptide to AB_{bt} (Figure 5B). In fact, most backbone NH frequencies showed the same ΔCS in the comparisons between HMGB1 and AB_{bt} and AB_{bt} plus or minus T-peptide (consider the symmetrical appearance of the two halves of Figure 4).

These results indicate that the acidic tail interacts with the boxes in the same way whether it is linked or not to the rest of the protein.

DISCUSSION

In the present study we tried to understand the structural relationship between the acidic tail and the HMG boxes of HMGB1. We show that in the context of the full-length protein the acidic tail is unstructured and interacts with specific residues in both boxes. This interaction is faithfully recapitulated by the interaction of a synthetic peptide and tailless HMGB1, indicating that it does not matter whether the acidic tail is connected to the boxes or not.

Our conclusion is based on the following evidence: (i) Tailless HMGB1 has a lower thermal stability than full-length HMGB1 but in the presence of T-peptide regains an identical stability to full-length HMGB1. The difference in melting temperature (12 K) implies a strong stabilizing effect of the acidic tail. (ii) NMR techniques identified residues in both boxes that interact either with T-peptide or with the acidic tail in the context of full-length HMGB1. In both cases, the boxes maintain their global fold and do not interact directly with each other. The acidic tail is unstructured in full-length HMGB1, like the T-peptide. The interactions between the boxes and the T-peptide are specific and not purely an effect of an unspecific electrostatic attraction, as a large number of basic residues dispersed throughout the boxes and the basic linker do not interact with the T-peptide.

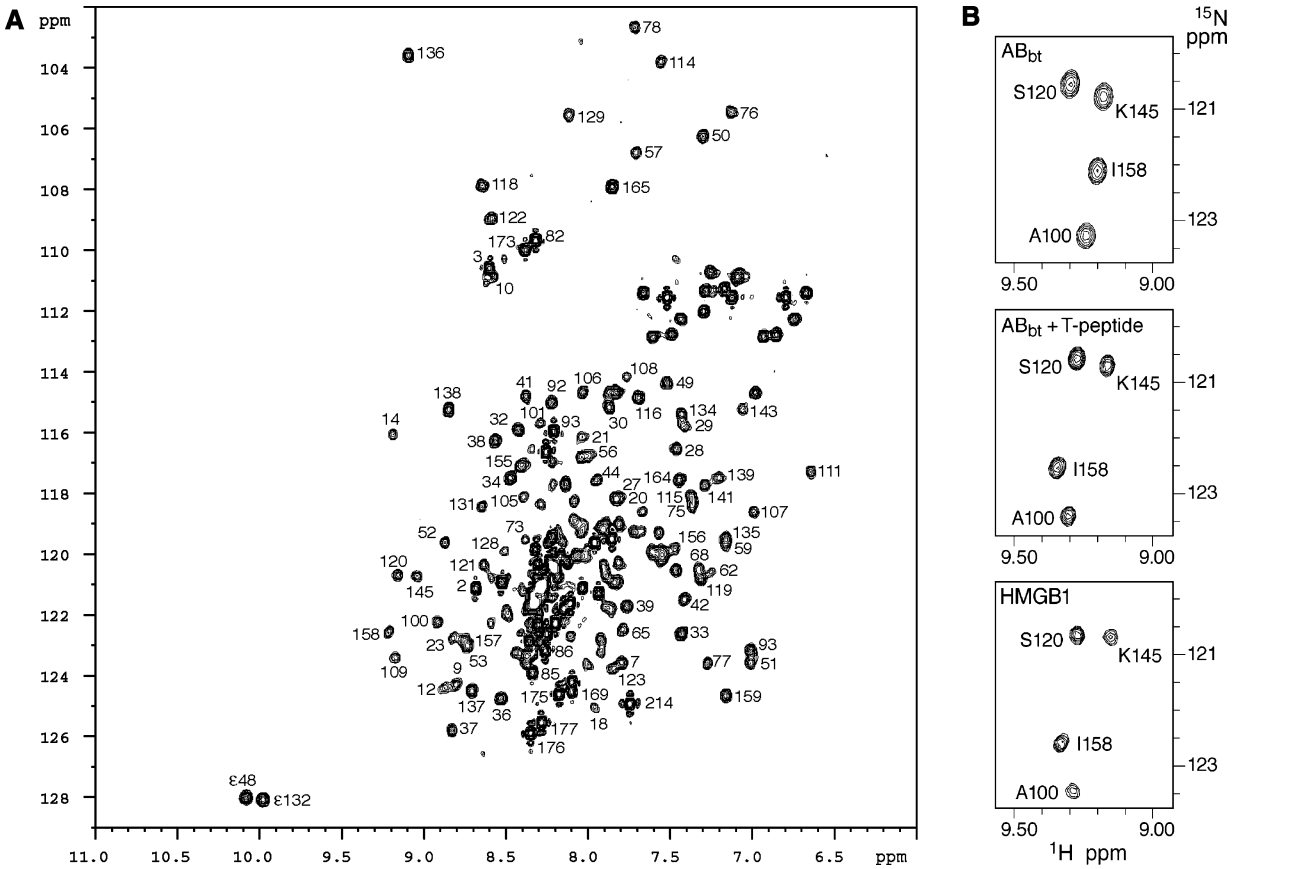

FIGURE 5: ^{1}H−^{15}N HSQC spectra. (A) ^{1}H−^{15}N HSQC spectrum of full-length HMGB1. Peaks are labeled with assignment information. In the region between 120 and 122 ppm (^{15}N) and 8.2−8.5 ppm (^{1}H) the sharp and intense peaks correspond to the unstructured acidic tail. Peaks in the region between 110 and 113 ppm (^{15}N) and 6.5−7.6 ppm (^{1}H) correspond to NH_2 side chains of Q and N residues. (B) Selected regions of the ^{1}H−^{15}N HSQC spectra of AB$_{bt}$ (top), AB$_{bt}$ complexed with T-peptide, 1:4 protein:peptide (middle), and full-length HMGB1 (bottom). Significant shifts in the peak position of residue I158 were observed when T-peptide or the acidic tail were present, whereas resonances S120, K145, and A100 did not move.

(iii) Isothermal calorimetry, circular dichroism, and sedimentation equilibrium experiments all indicate that box A and the T-peptide form a stable 1:1 complex. These techniques do not detect a stable complex between box B and the T-peptide, suggesting that the tail interacts more favorably with box A than with box B. Recent chemical cross-linking experiments have shown that the acidic tail interacts preferentially with box B (*22*). We note that we find interactions with both boxes; the nature of the cross-linking agent might have favored the formation of covalent bonds with box B rather than box A.

The basic stretch connecting box B with the acidic tail is also unstructured, as shown by the negative ΔCα chemical shifts and the absence of NOEs typical for secondary structures. Thus, we find no evidence of an additional α-helix, as proposed by Rauvala and collaborators on the basis of a proposed similarity between HMGB1 and S100 proteins (*7*, *31*). The sum of the basic stretch and the acidic tail creates an unusually long flexible extension, with an average length that exceeds the total size of both boxes. It is this flexible extension that binds to the HMGB1 receptor RAGE (*31*).

Our NMR binding studies reveal residues on the surface of the two HMG boxes that are in close proximity with the tail peptide. Despite the high positive surface potential, no interaction of the acidic tail was detected with helix III: backbone NH frequencies are not affected and neither are

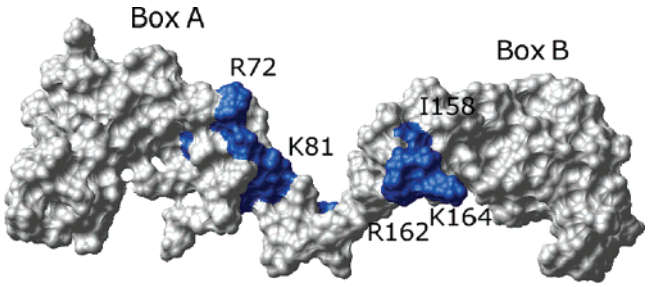

FIGURE 6: Schematic representation of HMGB1. Surface representation of a model of boxes A and B connected by their linker. The side chains of the residues displaying significant chemical shift differences (see Figure 4) are shown in blue. The boxes are rotationally free with respect with each other; therefore, the relative orientation of the two boxes has been chosen randomly. Note that the side chains in box A and box B that interact with the tail might come close to each other (as in this representation) and the tail might insert between them.

side-chain ϵNH frequencies of arginines. Thus, the interactions between the boxes and the tail peptide are not simply a result of an electrostatic attraction. Interestingly, the model of the AB$_{bt}$ fragment (Figure 6) suggests that the amino acids interacting with the tail may form the two walls of a canyon that has as the floor the linker connecting the boxes. Of course, Figure 6 only shows a static representation of a particular orientation between the boxes, which on the other hand behave as structurally independent entities. When the boxes are not in the relative orientation depicted in Figure

6, the tail may interact with a single box at a time.

The T-peptide−AB_{bt} system is in fast exchange, and the maximum proton chemical shift difference ($\Delta\delta$) observed for I158 is 78 Hz, yielding a lower limit of 500 s^{-1} for the dissociation rate constant k_{diss} ($k_{diss} \gg 2\pi\Delta\delta$; ref *32*). Therefore, the T-peptide has a maximal residence time of 2 ms in the complex with one or both boxes. According to our model, the interaction of the tail with the boxes in the full-length protein will be similar. Significantly, although the tail−box complex is a dynamic system, the tail will be in close proximity to the boxes most of the time and can shield them from other interactions. This can explain its role in modulating the interaction of HMGB1 with DNA and its helix-distorting ability (*14*−*17*), in reducing nucleosome binding (*18*), and in shielding Lys 81 in the linker between the two boxes from acetyltransferases (*20*). It is also likely that the acidic tail affects the cytokine function of HMGB1 by modulating interactions with receptors and plasma components. Conversely, the interaction of HMGB1 with DNA and/or other proteins can easily displace the acidic tail from the interaction with the boxes; the displaced tail might then assume a different role as a charged surface for additional interactions.

ACKNOWLEDGMENT

We thank Prof. J. Thomas for the generous gift of plasmid pT7-7-rHMG1cm, Laura Comelli for technical assistance, and Dr. Mark Pfuhl for useful discussions.

REFERENCES

1. Thomas, J. O., and Travers, A. A. (2001) HMG1 and 2, and related 'architectural' DNA-binding proteins, *Trends Biochem. Sci. 26*, 167−174.
2. Agresti, A., and Bianchi, M. E. (2003) HMGB proteins and gene expression, *Curr. Opin. Genet. Dev. 13*, 170−178.
3. Calogero, S., Grassi, F., Aguzzi, A., Voigtländer, T., Ferrier, P., Ferrari, S., and Bianchi, M. E. (1999) The lack of chromosomal protein HMG1 does not disrupt cell growth, but causes lethal hypoglycaemia in newborn mice, *Nat. Genet. 22*, 276−280.
4. Andersson, U. G., and Tracey, K. J. (2004) HMGB1, a pro-inflammatory cytokine of clinical interest: introduction, *J. Intern. Med. 255*, 318−319.
5. Müller, S., Scaffidi, P., Degryse, B., Bonaldi, T., Ronfani, L., Agresti, A., Beltrame, M., and Bianchi, M. E. (2001) The double life of HMGB1 chromatin protein: architectural factor and extracellular signal, *EMBO J. 20*, 4337−4340.
6. Hori, O., Yan, S. D., Ogawa, S., Kuwabara, K., Matsumoto, M., Stern, D., and Schmidt, A. M. (1995) The receptor for advanced glycation end products (RAGE) is a cellular binding site for amphoterin, *J. Biol. Chem. 270*, 25752−25761.
7. Huttunen, H. J., and Rauvala, H. (2004) Amphoterin as an extracellular regulator of cell motility: from discovery to disease, *J. Intern. Med. 255*, 351−366.
8. Read, C. M., Cary, P. D., Crane-Robinson, C., Driscoll, P. C., and Norman, D. G. (1993) Solution structure of a DNA-binding domain from HMG1, *Nucleic Acids Res. 21*, 3427−3436.
9. Hardman, C. H., Broadhurst, W. R., Raine, A. R. C., Grasser, K. D., Thomas, J. O., and Laue, E. D. (1995) Structure of the A-domain of HMG1 and its interactions with DNA as studied by heteronuclear three- and four-dimensional NMR spectroscopy, *Biochemistry 34*, 16596−16607.
10. Ohndorf, U. M., Rould, M. A., He, Q., Pabo, C. O., and Lippard, S. J. (1999) Basis for recognition of cisplatin-modified DNA by high-mobility-group proteins, *Nature 399*, 708−712.
11. Weir, H. M., Kraulis, P. J., Hill, C. S., Raine, A. R. C., Laue, E. D., and Thomas, J. O. (1993) Structure of the HMG box motif in the B-domain of HMG1, *EMBO J. 12*, 1311−1319.
12. Grasser, K. D., Teo, S. H., Lee, K. B., Broadhurst, R. W., Rees, C., Hardman, C. H., and Thomas, J. O. (1998) DNA-binding properties of the tandem HMG boxes of high-mobility-group protein 1 (HMG1), *Eur. J. Biochem. 253*, 787−795.
13. Ramstein, J., Locker, D., Bianchi, M. E., and Leng, M. (1999) Domain-domain interactions in high mobility group1 protein (HMG1), *Eur. J. Biochem. 260*, 692−700.
14. Sheflin, L. G., Fucile, N. W., and Spaulding, S. W. (1993) The specific interactions of HMG 1 and 2 with negatively supercoiled DNA are modulated by their acidic C-terminal domains and involve cysteine residues in their HMG 1/2 boxes, *Biochemistry 32*, 3238−3248.
15. Stros, M., Stokrová, J., and Thomas, J. O. (1994) DNA-looping by the HMG-box domains of HMG1 and modulation of DNA binding by the acidic C-terminal domain, *Nucleic Acids Res. 22*, 1044−1051.
16. Müller, S., Bianchi, M. E., and Knapp, S. (2001) Thermodynamics of HMG1 interaction with duplex DNA, *Biochemistry 40*, 10254−10261.
17. Lee, K.-B., and Thomas, J. O. (2000) The effect of the acidic tail on the DNA-binding properties of the HMG1,2 class of proteins: Insights from tail switching and tail removal, *J. Mol. Biol. 304*, 135−149.
18. Bonaldi, T., Längst, G., Strohner, R., Becker, P. B., and Bianchi, M. E. (2002) The DNA chaperone HMGB1 facilitates ACF/CHRAC-dependent nucleosome sliding, *EMBO J. 21*, 6865−6873.
19. Travers, A. A. (2003) Priming the nucleosome: a role for HMGB proteins?, *EMBO Rep. 4*, 131−136.
20. Pasheva, E., Sarov, M., Bidjekov, K., Ugrinova, I., Sarg, B., Lindner, H., and Pashev, I. G. (2004) In vitro acetylation of HMGB-1 and -2 proteins by CBP: the role of the acidic tail, *Biochemistry 43*, 2935−2940.
21. Bonaldi, T., Talamo, F., Scaffidi, P., Ferrera, D., Porto, A., Bachi, A., Rubartelli, A., Agresti, A., and Bianchi, M. E. (2003) Monocytic cells hyperacetylate chromatin protein HMGB1 to redirect it towards secretion, *EMBO J. 22*, 5551−5560.
22. Jung, Y., and Lippard, S. J. (2003) Nature of full-length HMGB1 binding to cisplatin-modified DNA, *Biochemistry 42*, 2664−2671.
23. Delaglio, F., Grzesiek, S., Vuister, G. W., Zhu, G., Pfeifer, J., and Bax, A. (1995) NMRPipe: a multidimensional spectral processing system based on UNIX pipes, *J. Biomol. NMR 6*, 277−293.
24. Bartels, C.-H., Xia, T.-H., Billeter, M., Güntert, P., and Wüthrich, K. (1995) The program XEASY for computer-supported NMR spectral analysis of biological macromolecules, *J. Biomol. NMR 5*, 1−10.
25. Grzesiek, S., and Bax, A. (1992) Improved 3D triple resonance NMR techniques applied to a 31 kDa protein, *J. Magn. Reson. 96*, 432−440.
26. Grzesiek, S., and Bax, A. (1993) The importance of not saturating water in protein NMR. Application to sensitivity enhancement and NOE measurement, *J. Am. Chem. Soc. 115*, 12593−12594.
27. Wittekind, M., and Mueller, L. (1993) HNCACB a high sensitivity 3D NMR experiment to correlate amide-proton and nitrogen resonances with the alpha-and beta-carbon resoances in protein, *J. Magn. Reson. B 1001*, 201−205.
28. Grzesiek, S., and Bax, A. (1992) Correlating backbone amide and side chain resonances in larger proteins by multiple relayed triple resonance NMR, *J. Am. Chem. Soc. 114*, 6291−6293.
29. Piotto, M., Saudek, V., and Sklenar, V. (1992) Gradient-tailored excitation for single-quantum NMR spectroscopy of aqueous solutions, *J. Biomol. NMR 2*, 661−664.
30. Carson, M. (1991) Ribbons 2.0, *J. Appl. Crystallogr. 24*, 958−961.
31. Huttunen, H. J., Fages, C., Kuja-Panula, J., Ridley, A. J., and Rauvala, H. (2002) Receptor for advanced glycation end products-binding COOH-terminal motif of amphoterin inhibits invasive migration and metastasis, *Cancer Res. 62*, 4805−4811.
32. Garrett, D. S., Seok, Y. J., Peterkofsky, A., Clore, G. M., and Gronenborn, A. M. (1997) Identification by NMR of the binding surface for the histidine-containing phosphocarrier protein HPr on the N-terminal domain of enzyme I of the *Escherichia coli* phosphotransferase system, *Biochemistry 36*, 4393−4398.

BI049364K